

10805

Session 2022

A3 TRANSMISSION AND DISTRIBUTION EQUIPMENT

PS1 – Decentralisation of T&D Equipment

Short circuit analysis of a Doubly Fed Induction Generator and their Impact on Generator Circuit Breakers**Karthik Reddy VENNA****Siemens AG****Germany****Karthikreddy.venna@siemens.com****Hong URBANEK****Siemens AG****Germany****hong.urbanek@siemens.com****Alois LECHNER****Andritz Hydro GmbH****Austria****Alois.lechner@andritz.com****SUMMARY**

With a continuous increase of the share of renewable energies in power generation market, there is a definite need of stable power generation method. Wind power and solar power are extremely variable and a large share of these resources in the energy market is a challenge for the stability of the transmission system, as well as security of supply for the consumers. There is a need for back up capacity to generate power during no wind or no sun and high demand, as well as a need for storage capacity for surplus power. Pumped storage power plants (PSPP) are considered as the most optimal solution for this problem. With this focus, variable-speed generators like doubly-fed induction generators (DFIG) have also gained increasing importance in pump-storage power stations since they present big advantages compared to the classical topology with a synchronous generator, such as the possibility to vary the power absorbed in pumping mode over a certain range by means of the speed of the pump, the ability

to respond much more dynamically to changes in power set point values and the possibility to avoid critical zones in pump operation by varying the speed of the machine.

A detailed analysis of short circuit behavior for these machines in PSPP application is not vastly available. Mainly the effect of crowbar resistor which influences the current fed by DFIG in terms of AC and DC component is very important to consider when defining the requirements of a generator circuit breaker (GCB). The newly introduced dual logo standard IEC/IEEE 62271-37-013 FDIS version discusses about this application in Annex K but in a simplified manner. Various factors that affect the short circuit current curves like, rotor voltage, time varying crowbar resistor and the influence of external arc fault voltage in degree of asymmetry has not been discussed in detail. Since these factors have shown non negligible impact on the fault currents behavior, we have decided to explain them here.

This paper discusses about how a GCB with vacuum switching technology and with its arc characteristics can influence the fault interruption behavior and is able to handle the resulting short circuit currents even with a higher degree of Asymmetry and delayed current zeros making them a suitable protection technique for such high efficiency PSPPs. Typical DFIG machine data are considered as a case study and the impact of machine short circuit currents on generator circuit breaker shown in this paper.

KEYWORDS

DFIG, Vacuum Generator Circuit Breaker, Crowbar resistor, Delayed current zeros, Pumped Storage Power plants

1. INTRODUCTION

The pumped storage power plants (PSPP) are one of the commercially proven methods available for grid-scale energy storage. Building additional PSPPs particularly in the areas with high installed capacities of wind parks and solar power plants will significantly improve the grid reliability and operability. In order to ensure such reliability, the availability of the power plant must be high. In addition, variable-speed generators like DFIGs are showing promising performance in bigger storage power stations due to their enhanced flexibility with dynamical response to power demand. The generator circuit breakers (GCB) which are installed mainly to increase the availability of power plants must cope-up with additional challenges by variable speed machines. High number of switching operations, frequent switching with load currents, interrupting short circuit currents with high degree of asymmetry are some to mention. Thus, the installed GCBs must be able to handle such additional stresses in order to protect the generator & step-up transformer which represent the generating asset and whose availability is of high stake for the PSPP revenues. Vacuum Generator Circuit Breakers (VGCB) which are available for short circuit currents up to 110 kA & rated currents up to 14000 A are investigated in this paper regarding their suitability in handling the stresses mentioned above that are additional to the stresses mentioned in the standard IEC-IEEE 62271-37-013.

This paper deals with explaining a typical short circuit behavior of a DFIG and how they pose additional challenges on generator circuit breakers. With the help of a case study of a typical DFIG machine, it is shown why an individual short circuit analysis is needed for such machines and how VGCBs are ideally suitable for such applications with its interruption capabilities.

2. DFIG SHORT CIRCUIT BEHAVIOR

A PSPP with variable speed machine uses a reversible hydro turbine to store the electrical energy by pumping the water from a lower reservoir to a higher reservoir during the time when the demand of the load is low and it pumps or generates the electricity by allowing the water from higher reservoir to a lower reservoir during the period of time when the demand of power is high. Today, the maximum efficiency of a DFIG is about 85% [1]. The stator of DFIG is connected to the grid through a transformer while the rotor of DFIG is connected to adjustable blade hydro turbine and a power electronics converter is used to control the speed of the DFIG as shown in the Fig. 1

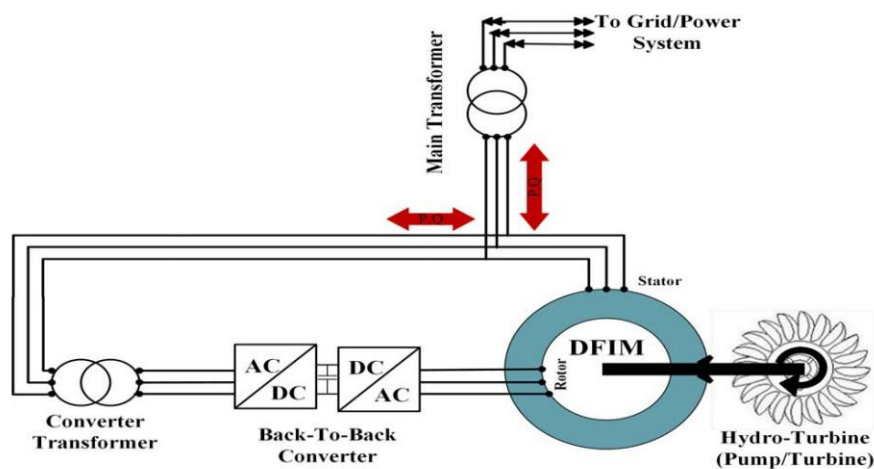


Fig. 1 PSPP using DFIG fed by a back-to-back power electronics converter [2]

For a variable-speed PSPP, the short-circuit current can be determined relatively easily. It is determined by the converter and will generally not exceed the nominal current of the converter [3]. The short-circuit behavior of induction machines is strongly dependent on the machine characteristics. It has received considerable attention in the past and some good approximate equations to determine the maximum short-circuit current have been derived.

A DFIG is also directly coupled to the grid but it has a power electronic converter connected between the rotor windings of the induction machine and the grid. It needs to have a provision to protect the converter during short circuits [4]. The voltage drop at the terminals will result in large, oscillatory currents in the stator windings of the DFIG. Because of the magnetic coupling between stator and rotor, these currents will also flow in the rotor circuit and through the converter system. The high currents can cause thermal breakdown of the converter. Thus, crowbar resistors are used to limit these short circuit currents. During a fault, the rotor windings are short-circuited by a set of resistors. The short-circuit current will flow through this crowbar instead of the converter.

One of the most important criteria of selecting the crowbar resistance value is to find an optimum balance between limiting the short circuit current below the thermal break down level of the converter system and at the same time not leading to very high voltage drop across the converter terminals which could also lead to converter damage.

The equivalent circuit of a DFIG is shown in Fig. 2, which is basically the same as the equivalent circuit of a transformer. A detailed analyses of the characteristics of the current fed by a DFIG after a three-phase short-circuit at its terminals are documented in many publications [4], [5], [6].

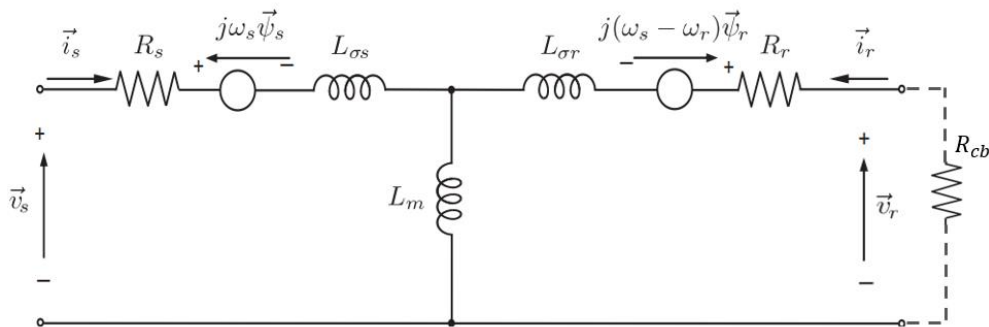


Fig. 2 Equivalent circuit of a DFIG machine

When a three-phase short circuit occurs at stator terminals, it is important to mention that the dc component of the fault current decays with the stator time constant T'_S while the decaying of the ac amplitude is influenced by the rotor time constant T'_R as shown below. The relevant formulae are explained in detail [4].

$$L'_S = L_{\sigma S} + \frac{L_{\sigma R} \cdot L_m}{L_{\sigma R} + L_m} \quad T'_S = \frac{L'_S}{R_S} \quad L'_R = L_{\sigma R} + \frac{L_{\sigma S} \cdot L_m}{L_{\sigma S} + L_m} \quad T'_R = \frac{L'_R}{R_R}$$

However, similar to the transformer principle, the crowbar resistance value used on rotor side, needs to be calculated to the stator reference while calculating rotor time constant and its contribution in decay of AC component on stator contribution to short circuit current. Fig. 3 shows the difference in short circuit currents based on crowbar resistance value when correctly referred to stator side and not.

$$R_{cbS} = R_{cb} \times \left(\frac{U_S}{U_R}\right)^2 \quad \text{with} \quad T'_R = \frac{L'_R}{R_R + R_{cbS}}$$

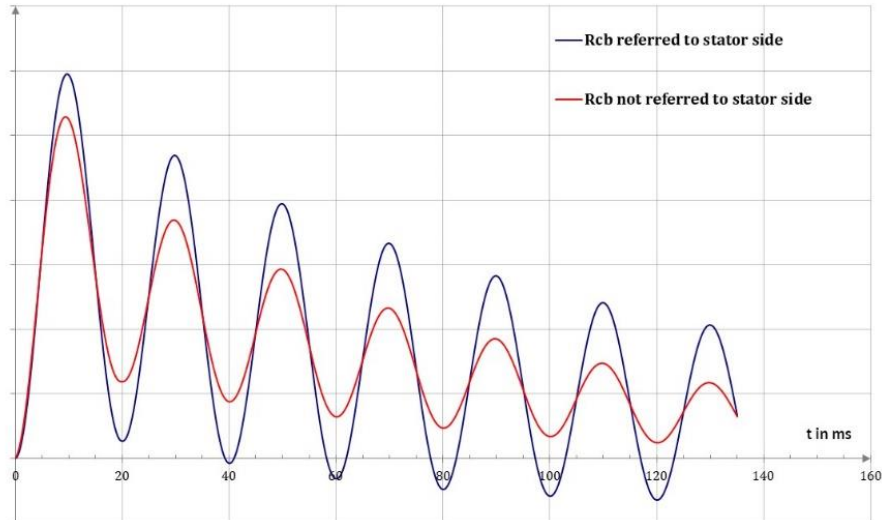


Fig. 3: Short circuit currents when crowbar resistance is referred to the correct side

The crowbar is a protective device which is only needed when the back-to-back converter connected to the rotor is overloaded either with DFIG rotor voltage or DFIG rotor current. This situation occurs when the DFIG stator voltage changes rapidly, e.g. when a short circuit near to the stator appears.

There are different approaches for applying the crowbar, both in timing and crowbar resistance. One is to have a high value crowbar resistance R_{cb1} at the beginning of the short-circuit occurrence. High values of the crowbar resistance have the advantage of fast decay of the rotor DC component, which reduces the duration for having the converter out of operation. On the other hand, a very fast decaying AC can lead to missing current zeroes which poses a problem for every medium voltage switching device – independent of their switching media. If the current is so high that the converter is unable to resume current control in reasonable time and the DFIG has to be switched off, a second crowbar stage is implemented with a very low resistance R_{cb2} .

The other approach is to design and dimension the converter to reduce the crowbar activity to a range in which DFIG must be switched off anyhow. In this case, the crowbar resistance values are usually very small resulting in similar stator AC and DC time constants, which is similar to typical induction machines.

3. VACUUM GENERATOR CIRCUIT BREAKERS (VGCB)

Today more than 80% of the switching devices installed in the medium voltages from 7.2 kV up to 52 kV are vacuum circuit breakers due to their many advantages over other existing technologies. Until the end of 90's, it was not possible to utilize the potential of this long proven vacuum technology for the generator switching applications even though they fall under medium voltage applications. The only suitable switching technology used for the generator applications was using SF6 as an arc quenching medium. But the technological developments in the field of vacuum arc physics enabled the VGCBs to interrupt high short circuit currents up to 110 kA and carry high continuous currents up to 14000 A. Schramm & Kulicke [7] are the first who stated that the VGCBs are suitable to clear the fault currents with delayed current zeros and are able to withstand very high current amplitudes resulting from the high DC components up to > 100% with possible delayed current zeros. At such a high degree of asymmetry, the vacuum contacts must be able to withstand the thermal stress due to the longer

arc duration and still be able to interrupt the fault current. The most commonly used contact types for VGCBs are AMF (Axial Magnetic Field) contacts as shown in the Fig. 4. When the vacuum arc is created and the current is passed through the contacts, the higher amplitudes of the current make the arc constricted and due to the presence of axial magnetic field from the contact design the arc is forced to diffuse over the entire surface of the contact.

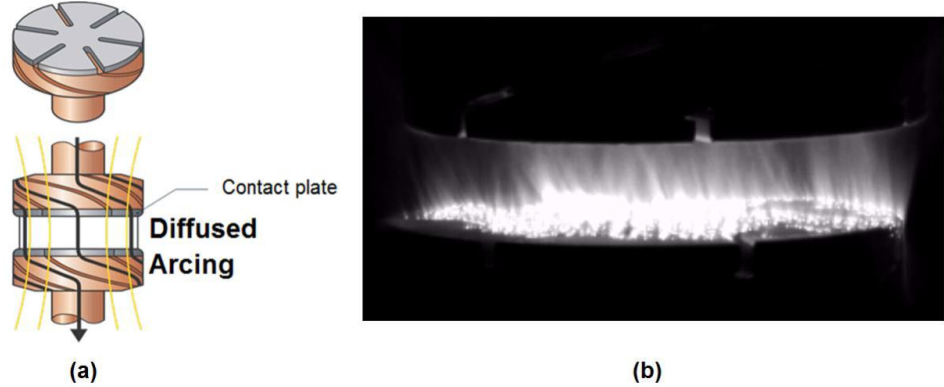


Fig. 4 (a) AMF contact design, (b) Diffused arc on the contact surface

The arc voltage due the diffused arc between AMF contacts is considerably low but it does have a noticeable effect on the DC decaying behavior of short-circuit current in generator circuits, especially in case of generator-source current. Recent measurements show that the arc voltage for AMF contact types (diffuse arc) is in the range of 80 – 120 V recorded in internal tests.

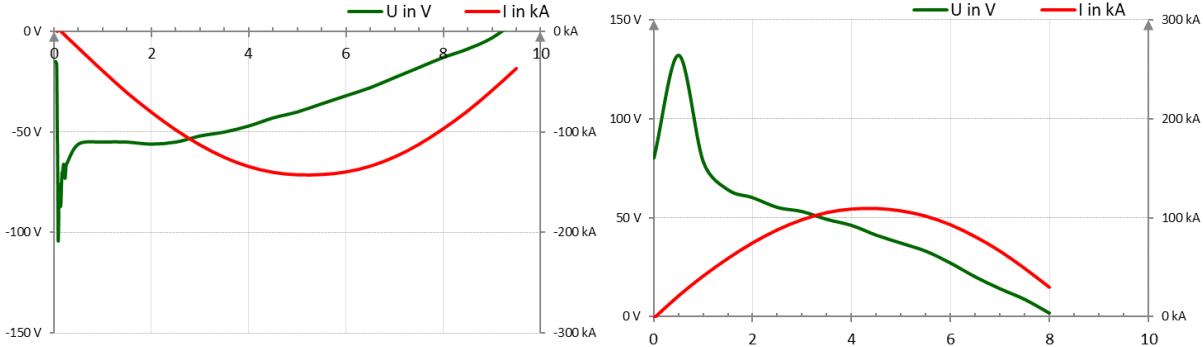


Fig. 5 arc voltage for AMF contacts

The resistive character of an arc (r_{arc}) can reduce the DC time constant after the contact parting leading to a positive effect on the decaying of the DC offset and reduce the arcing time significantly as shown in Fig.6. Specific simulations were performed with 100 V of arc voltage and presented in [8].

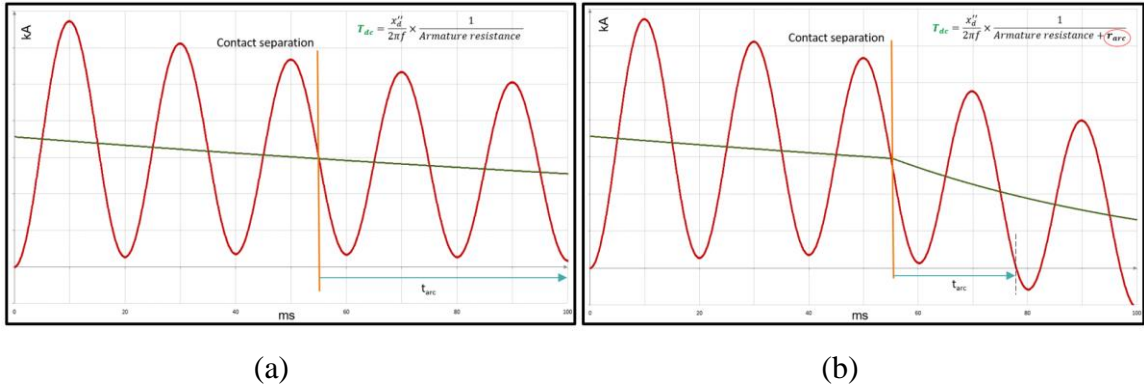


Fig. 6 without arc resistance (a) & effect of external arc resistance (b) on reducing arcing time

This leads to a significantly high number of switching operations for VGCBs – both load current (maintenance-free up to 10,000 CO operations and more) and short-circuit current (>30 operations at full short-circuit current rating). This makes VGCBs as ideal switching device for applications with very high amount of switching operations such as pump storage, where load current is switched very often. Refer to fig 7.

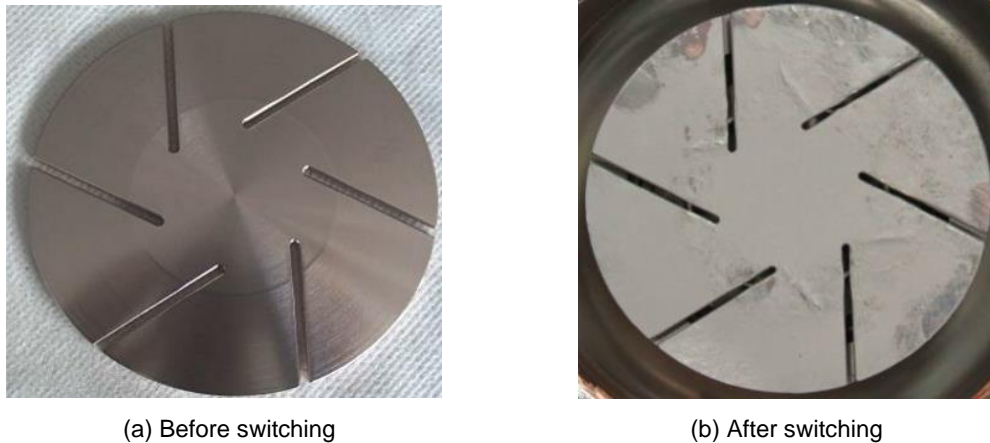


Fig. 7 Contact erosion on AMF contacts before & after switching 30 times of 80 kA short circuit current

Also the low contact erosion and the diffused arc is the reason why the VGCBs can handle long arcing times. This characteristic is important as the main challenge on GCBs while switching DFIGs is the prolonged arcing time when compared to a traditional synchronous generator. This is verified through tests at KEMA [10] where GCBs have been tested with arcing times of up to 80 ms. This is further supported by the extensive experience of VCBs installed in German railway networks where the operating frequency is 16.7 Hz which are typically tested with long arcing times.

Further in GCB networks, TRVs have a very steep rate of rise of recovery voltages. In order to cope up with such steep TRVs, an additional capacitance between the transformer and the GCB is used to reduce the rate-of-rise of the transient recovery voltage from the application. As a result, the slope of the TRV is lowered. However, vacuum as dielectric medium has a very fast recovery strength in the range of $> 10 \text{ kV}/\mu\text{s}$ [9] and therefore can easily withstand the required high TRV and RRRV of generator applications. Thus, the need of the additional capacitors is eliminated by VGCBs.

4. CASE STUDY

In this section the case of a three-phase fault at the stator terminals of a typical DFIG (Table. 1) used in a PSPP is simulated using the Electromagnetic Transients Method. Simulations are primarily focused to show the influence of different crowbar resistance value and different available crowbar implementation philosophies. Also, since the excitation of a synchronous generator is usually connected to the generator stator, the grid-side connection of the back-to-back-converter is always connected to the main transformer and thus being in service. As a result, there is no possibility for the GCB to close into a short-circuit. So, it is also considered during the simulations that the three-phase short circuit occurs only when GCB is closed position and generator is underload. Thus, as stated in the dual logo standard IEC / IEEE 62271-37-013 an external arc fault voltage of 300 V is considered in the calculations from the instance of short-circuit inception.

Different crowbar resistance values (R_{cb1}) mentioned in Table2 are used for the machine parameters listed in Table 1 to see their individual influence on the arcing time with external fault voltage and without external fault voltage plotted in Fig. 8. Further the influence of time-based crowbar switching philosophy using R_{cb2} is also simulated, and the results are plotted at two scenarios – a. When fault initiated at Voltage Max and b. fault initiated and Voltage zero plotted in ANNEX - I.

Table 1: DFIG Parameters

Rated apparent power	S_r	MVA	280
Stator Rated voltage	U_s	kV	15.0
Rated current	I_r	A	10777
Transformation ratio	U_s/U_r		0.62
Stator leakage reactance	$X_{S\sigma}$	p.u	0.125
Rotor leakage reactance	$X_{R\sigma}$	p.u	0.165
Magnetizing reactance	X_m	p.u	2.260
Stator resistance	R_s	p.u	0.0018
Rotor resistance	R_r	p.u	0.0016
Crowbar resistance	R_{cb1}/R_{cb2}	m Ω	Table 2

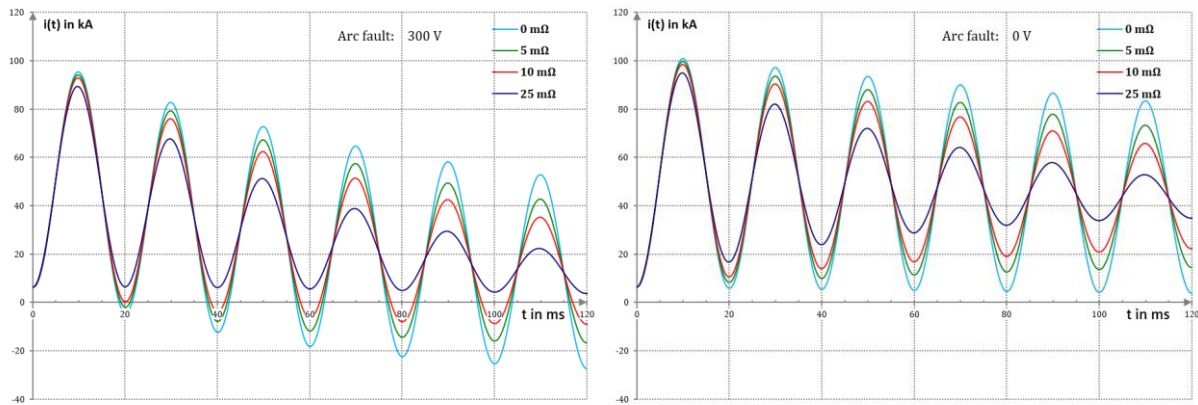
Table 2: R_{cb1} & R_{cb2} values

Cases	R_{cb1}	R_{cb2}
1	0 m Ω	n.a
2	5 m Ω	n.a
3	10 m Ω	n.a
4	25 m Ω	n.a
5	25 m Ω	10 m Ω
6	25 m Ω	5 m Ω

The following results are observed.

Table 3: Calculation results with external arc voltage

Cases	R_{cb1}	R_{cb2}	I_{sym}	DC%	i_p	t_{arc}
1	0 m Ω	0 m Ω	30,9 kA	61 %	95 kA	8 ms
2	5 m Ω	0 m Ω	26,7 kA	71 %	94 kA	8 ms
3	10 m Ω	0 m Ω	23,1 kA	82 %	93 kA	7 ms
4	25 m Ω	0 m Ω	14,9 kA	128 %	89 kA	45 ms
5	25 m Ω	10 m Ω	19,6 kA	96 %	89 kA	6 ms
6	25 m Ω	5 m Ω	21,6 kA	88 %	89 kA	7 ms



a) with external fault voltage (300 V) b) without external voltage (0 V)

Fig. 8: effect of crowbar resistance with and without external arc voltage

5. CONCLUSION

DFIGs have recently considered as efficient alternative in pump-storage power stations due to their many advantages compared to the classical topology with a synchronous generator. Therefore, a deep understanding of the characteristics of the fault current fed by a DFIG after a three-phase short-circuit at its terminals is very important while dimensioning the GCB that is installed to protect both step up transformer and generator.

In addition, with the help of a typical DFIG machine various faults current scenarios fed by a DFIG are presented also with focus on crowbar resistance due to the fact that they impose very severe stresses for a GCB with respect to the degree of asymmetry. Additionally, the effect of external arc voltage on short circuit current behavior is considered stated in the standard IEC / IEEE 62271-37.013 and showed the positive impact of it on arcing time of the circuit breaker. At the end it is clear that a short circuit analysis is always required for such DFIG machine while selecting a suitable GCB and so far, VGCB technology showed promising performance being able to clear the faults and increase protection for such DFIG operated PSPPs.

BIBLIOGRAPHY

- [1] Jiaqi Liang, Harley and R.G., "Pumped Storage Hydro-Plant Models for System Transient and Long-Term Dynamic Studies," Presented at IEEE Power and Energy Society General Meeting, 2010, pp. 1-8.
- [2] U. Nasir, Z. Iqbal, M. T. Rasheed et al., "Active and reactive power control of a variable speed pumped storage system", *2015 IEEE 15th International Conference on Environment and Electrical Engineering (EEEIC)*, pp. 6-11, 2015.
- [3] J. Morren, J. T. G. Pierik, and S. W. H. de Haan, "Voltage dip ride-through of direct-drive wind turbines," presented at the 39th Int. Univ. Power Eng. Conf., Bristol, U.K., Sep. 6–8, 2004.
- [4] J. Morren and S. W. H. de Haan, "Ridethrough of wind turbines with doubly-fed induction generator during a voltage dip," *IEEE Trans. Energy Convers.*, vol. 20, no. 2, pp. 435–441, Jun. 2005.
- [5] A. Marmolejo, M. Palazzo, M. Delfanti. Short-Circuit Current of a Doubly-Fed Induction Generator: Analytical Solution and Insights. *IEEE Conference on Energy Conversion (CENCON)*, 2014.
- [6] Xueguang Zhang, Rui Li, Dianguo Xu. Analysis of three-phase short circuit current of DFIG. *Power Electronics and Applications, 2009. EPE '09. 13th European Conference*.
- [7] B. Kulicke, H. H. Schramm, "Application of Vacuum Circuit-Breaker to Clear Faults with Delayed Current Zeros", *IEEE Trans. Power Delivery*, vol.3, no.4, Oct.1988, pp.1714-1723
- [8] K. R. Venna, N. Anger, T. Kleinert, "Role of vacuum generator circuit breaker in improving the plant efficiency & protecting the generators up to 450 MVA", *Power Gen- EU*, 2016
- [9] K. R. Venna, H. Urbanek, N. Anger, "Difference between Switching Of Motors & Generators with Vacuum Technology", Paper 0872, *CIGRE* 2017
- [10] Test Report of Performance TIC 2476-12, KEMA, 2012.

ANNEX - I

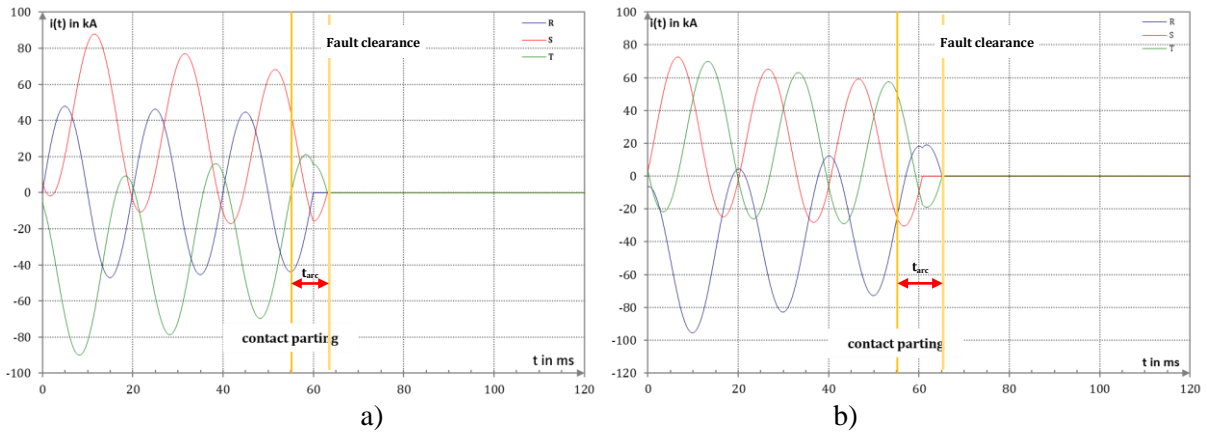


Fig. 9 current curve case 1: $R_{cb1} = 0 \text{ m}\Omega$, $R_{cb2} = 0 \text{ m}\Omega$
 a) fault initiation at voltage maximum b) fault initiation at voltage zero

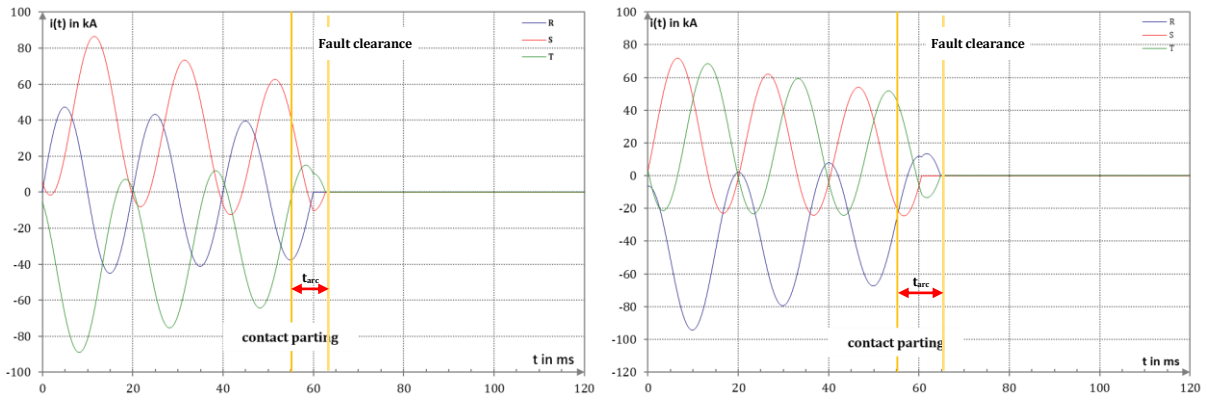


Fig. 10 current curve case 2: $R_{cb1} = 5 \text{ m}\Omega$, $R_{cb2} = 0 \text{ m}\Omega$
 a) fault initiation at voltage maximum b) fault initiation at voltage zero

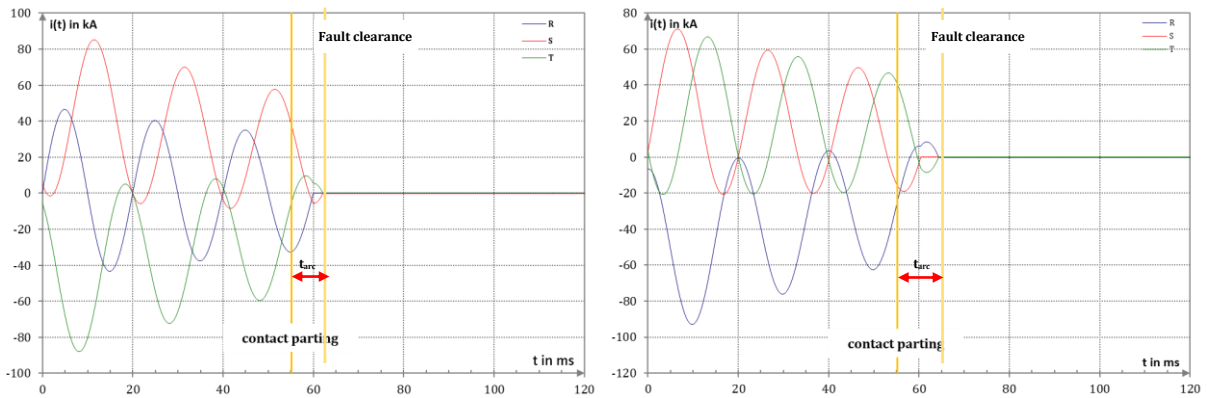


Fig. 11 current curve case 3: $R_{cb1} = 10 \text{ m}\Omega$, $R_{cb2} = 0 \text{ m}\Omega$
 a) fault initiation at voltage maximum b) fault initiation at voltage zero

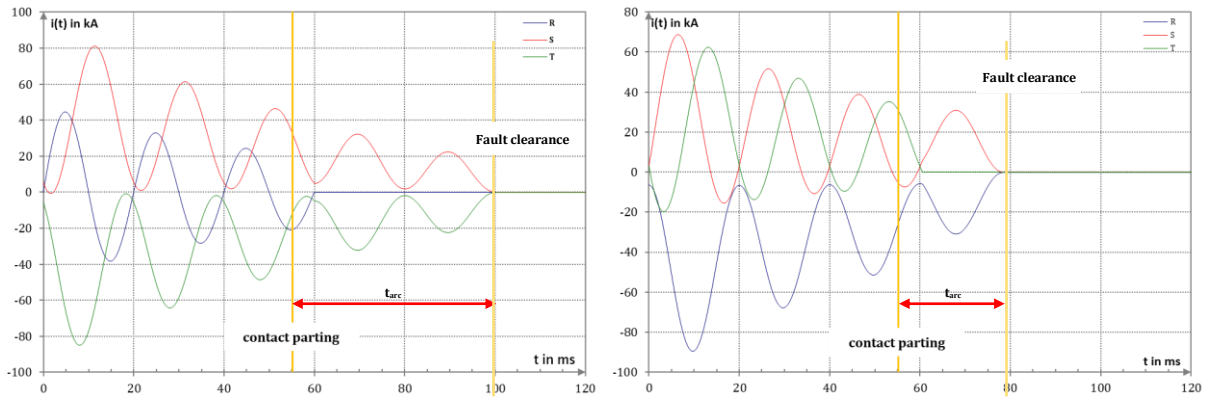


Fig. 12 current curve case 4: $R_{cb1} = 25 \text{ m}\Omega$, $R_{cb2} = 0 \text{ m}\Omega$
 a) fault initiation at voltage maximum b) fault initiation at voltage zero

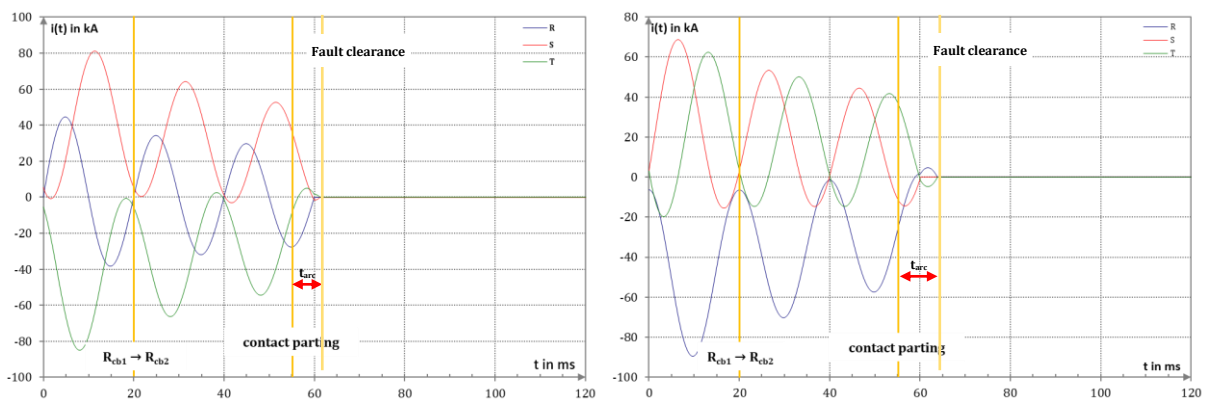


Fig. 13 current curve case 5: $R_{cb1} = 25 \text{ m}\Omega$, $R_{cb2} = 10 \text{ m}\Omega$
 a) fault initiation at voltage maximum b) fault initiation at voltage zero

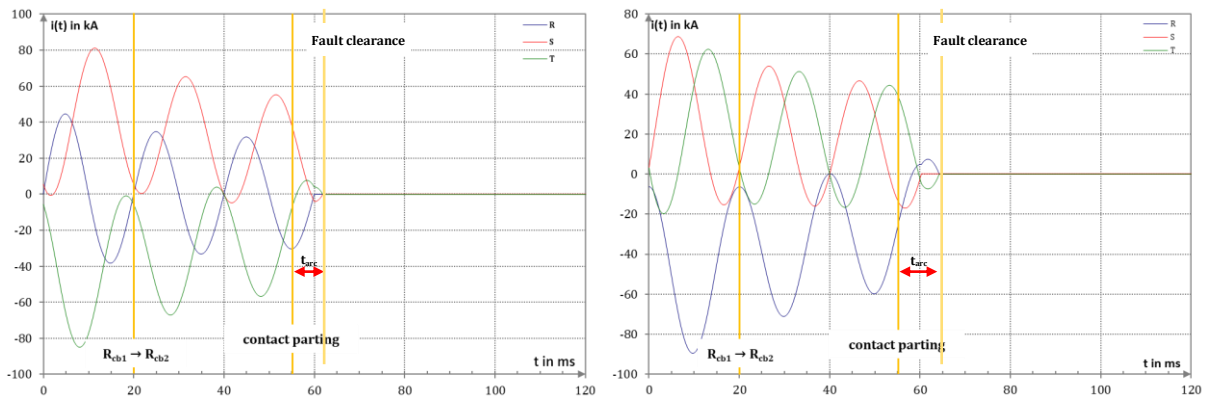


Fig. 14 current curve case 6: $R_{cb1} = 25 \text{ m}\Omega$, $R_{cb2} = 5 \text{ m}\Omega$
 a) fault initiation at voltage maximum b) fault initiation at voltage zero